

Mathematical model of solid tumor formation

R.G.Khlebopros¹, V.A.Slepkov², V.G.Sukhovolsky², Y.V.Mironov^{2,3}, V.E.Fedorov³, S.P.Gabuda^{3*}

¹*Institute of Biophysics, KSC SB RAS, Akademgorodok, Krasnoyarsk, 660036, Russia*

²*International Centre for Critical States Research, KSC SB RAS, Akademgorodok, Krasnoyarsk, 660036, Russia*

³*Nikolayev Institute of Inorganic Chemistry of Siberian Department of Russian Academy of Sciences. Novosibirsk 630090, Russian Federation*

*) Corresponding author: gabuda@casper.che.nsk.su

Abstract. The problem of the onset and growth of solid tumour in homogeneous tissue is regarded using an approach based on local interaction between the tumoral and the sane tissue cells. The characteristic sizes and growth rates of spherical tumours, the points of the beginning and the end of spherical growth, and the further development of complex structures (elongated outgrowths, dendritic structures, and metastases) are derived from the assumption that the reproduction rate of a population of cancer cells is a non-monotone function of their local concentration. The predicted statistical distribution of the characteristic tumour sizes, when compared to the clinical data, will make a basis for checking the validity of the theory.

Key words: tumour growth, mathematical model, local interaction

1. Introduction

Tumour growth modelling has been the subject of much recent literature (e.g., [1-12]), but the existing mathematical models appear to neglect the local interaction between cancer and tissue cells. This interaction between cancer and tissue cells affects the cancer cells' reproduction rate the way that it becomes dependent on their local concentration [13-17]. Therefore, tumour growth is mainly determined by the behaviour of cancer cells adjacent to the tumour surface. This process, in its turn, is largely dependent on the tumour's local curvature. We apply this approach to investigate the macroscopic effects of tumour growth in a homogeneous tissue. The effects of local interaction can be most simply described using the reproduction function approach. Figure 1 shows hypothetical non-monotone curves 1-3 describing the reproduction rate of cancer cells $\dot{\nu}$ vs. local concentration $\nu = \frac{x}{x+y}$, where x and y are the number of cancer and tissue cells, respectively, in

the considered tissue area. (For simplicity and without loss of generality, cancer and tissue cells are assumed hereafter to be of the same size). The curves represent the interaction of carcinogenic factors with the immune system, the availability of nutrients, and the local cellular interaction. On each plot, the first interval of decrease corresponds to the activation of the immune system in response to the presence of cancer cells in the organism. The same behaviour is expected when the immune system in affected organism is supported by definite antitumoral medicines. Among them are widely known antioxidants like selenium. The series of methods as aimed in direct damage of cancer cells. The newest is the use of some radioactive-isotope containing complexes employed for treatment of different cancer diseases - from kidney, lung and stomach to brain and bones [18-21]. Very recently, in medical practice is widely used the photo dynamic therapy (PDT) based on the luminescence of introduced preparation which can activate oxygen and destroy the tumor cells. We suppose that this phenomenon is of special interest for rhenium complexes: the combination of metal cluster luminescence and of metal radioactivity (the ¹⁸⁶Re and ¹⁸⁸Re radioactive isotopes) can create synergetic effect in cancer therapeutics. The use of similar improved methods for tumour treatment need in detailed modelling of the tumour growth.

Furthermore, as the concentration of cancer cells increases, the suppression of their reproduction through local interaction between cancer and tissue cells is first slowed, then completely stopped. Finally, it gives way to a reverse process in which cancer cells stimulate the pathological division of the tissue cells [14, 15]. On the plots, this process corresponds to the interval of increase. A still higher concentration of cancer cells causes a deficit of nutrients which results in the inhibition of cancer cells' reproduction rate and finally to their death. On the plots, this process corresponds to the second interval of decrease.

Curve 1 describes the case when tumour onset in the tissue is fully suppressed. When the immune system cannot provide complete suppression (curve 2), tumours can spontaneously arise and develop. This case is the subject of our study. Curve 3 images a suppressed immune system when the tumour spreads throughout the organism.

2. Growth and formation of solid tumours

For the sake of simplicity we are solving this problem in two dimensions which corresponds to the behaviour of tumour sections. The difference between the three- and two-dimensional formulations is of minor importance as we consider the processes only qualitatively. Assume that the reproduction function is given by $\dot{\nu} = \varphi(\nu)$, R is the radius of a spherical tumour, and r is the radius of cancer and tissue cells. Define the density ν of cancer cells in the vicinity of the surface as $\frac{S_c}{S_c + S_t}$, where $S_c = 4\pi r(R - r)$ is the area of a layer of tumour cells that contact the surface from inside, and $S_t = 4\pi r(R + r)$ is the area of a layer of tissue cells that contact the surface from outside:

$$\nu = \frac{R - r}{2R}. \quad (1)$$

R and \dot{R} are found from (1) as

$$R = \frac{r}{1 - 2\nu}, \quad (2)$$

$$\dot{R} = \frac{2r\dot{\nu}}{(1 - 2\nu)^2}. \quad (3)$$

Let a tumour occupy the area $V = 2\pi R^2$. Then

$$\dot{V} = 2\pi R\dot{R}. \quad (4)$$

On the other hand, \dot{V} is the area of cancer cells produced per unit time in the area $S_c + S_t$. Therefore

$$\dot{V} = (S_c + S_t)\varphi(\nu) = 8\pi r R \varphi(\nu), \quad (5)$$

From (4) and (5) obtain

$$\dot{R} = 4r\varphi(\nu).$$

Substituting the latter equation in (3) obtain differential equation for the density of cancer cells in the tumour's surface layer:

$$\dot{\nu} = 2\varphi(\nu)(1 - 2\nu)^2 = \psi(\nu). \quad (6)$$

Figure 2 shows the plot of $\psi(\nu)$ (solid line) compared with the plot of $\varphi(\nu)$ (dashed line).

From (2) find the minimum (R_{\min}) and the maximum (R_{\max}) radiuses of a spherical tumour and the critical value (R_t) above which the tumour begins to grow until it reaches R_{\max} :

$$R_{\min} = R_1 = \frac{r}{1 - 2\nu_1}, \quad R_t = R_2 = \frac{r}{1 - 2\nu_2}, \quad R_{\max} = R_3 = \frac{r}{1 - 2\nu_3}.$$

Radius $R_0 = R(\nu_0)$ (ν_0 is the maximum point) corresponds to the highest growth rate of cancer cells in the tumour's surface layer.

Between R_2 and R_0 the spherical shape of the tumour is stable against minor deformations of the surface curvature. When the sphere is extended into an ellipsoid, the areas with a smaller curvature radius tend to grow more slowly while the areas with a larger curvature radius grow faster, and the

tumour thus recovers its spherical shape (Fig. 3a). When the initial tumour radius is between R_0 and R_3 , the spherical shape of the tumour becomes unstable as the growth rate is inversely proportional to the curvature radius – and the tumour becomes extended into an ellipsoid (Fig. 3b). The further evolution can follow several scenarios. As long as the curvature radius at the sharp end of the ellipsoid exceeds R_0 it remains the site of the highest reproduction rate and extends more and more transforming the tumour into an elongated outgrowth (Fig. 3c). When the curvature radius at the sharp end of the outgrowth becomes smaller than R_0 , the sites of fastest reproduction remove along the sides of the stem to the points of curvature radius $R = R_0$ which causes new outgrowths and transforms the tumour into a dendritic structure (Fig. 3d). Later on the new outgrowths may detach from the main stem in the region of negative curvature corresponding to a negative growth of cancer cells (Fig. 3e). If a negative curvature develops at the junction of the outgrowth with the main tumour, the outgrowth may also detach and evolve as a separate metastasis (Fig. 3f).

3. Statistical distribution of tumours

3.1. General case

First consider the statistical distribution of tumours in a general case. Let the spontaneous onset of a tumour with the radius $R = R(v)$ in the tissue be given by the probability density $\eta(v)$, and the rate of density growth in the tumour's surface layer be given by

$$\dot{v} = \psi(v), \quad (7)$$

where v is between v_1 and v_2 . Find the average probability density $p(v)$ which is the distribution of tumours in the tissue in the time T elapsed after the beginning of the process. Let the general solution of (7) be

$$v = \bar{v}(t, v_0), \quad (8)$$

where v_0 is v at the initial time $t = 0$ and $v_1 \leq v_0 \leq v_2$. From (8) obtain

$$dv = \frac{\partial \bar{v}}{\partial v_0} dv_0 \quad (9)$$

for each fixed moment t . As the interval dv is the image of the interval dv_0 , the probabilities of these intervals are equal:

$$\eta(v) dv = \eta(v_0) dv_0, \quad (10)$$

where $v_1 \leq v \leq v_2$, $v_1 \leq v_0 \leq v_2$ and $v = \bar{v}(t, v_0)$. From (9) and (10) obtain

$$\eta(v) \frac{\partial \bar{v}}{\partial v_0} dv_0 = \eta(v_0) dv_0. \quad (11)$$

Assume that at each moment t the function v has the reverse function

$$v_0 = \bar{v}_0(v, t),$$

and rewrite (11) as

$$\eta(v) = \frac{\partial \bar{v}_0}{\partial v} \eta(v_0). \quad (12)$$

Then the equation for the probability density at the point v at the moment t is

$$p(v, t) = \begin{cases} \frac{\partial \bar{v}_0}{\partial v} \eta(\bar{v}_0(v, t)), & v \in [\bar{v}(t, v_1), \bar{v}(t, v_2)] \\ 0, & v \notin [\bar{v}(t, v_1), \bar{v}(t, v_2)] \end{cases}. \quad (13)$$

The probability $p(v)$ is found by integrating $p(\dot{v}, t)$ with respect to t over 0 to T :

$$p(v) = \frac{1}{T} \int_0^T p(v, t) dt, \quad v_1 \leq v \leq v_2. \quad (14)$$

3.2. Specific model

As only a qualitative description is supposed, specify $\eta(v)$ and $\psi(v)$ as the simplest functions with the required properties. Thus the function $\eta(v)$ (the probability density that a tumour with the radius $R = \frac{r}{1-2v}$ arises spontaneously in the tissue) must reach its maximum at zero and decrease rapidly.

Assume that

$$\eta(v) = e^{-v}. \quad (15)$$

Note that the density $v=0$ corresponds to the radius $R=r$ and $v=1/2$ corresponds to $R=\infty$. Let $\psi(v)$ be represented by a piecewise linear function $\dot{v} = \chi(v)$ (Fig. 4.), assuming for simplicity and without loss of generality that

$$v^1 = \frac{v_1 + v_2}{2}, \quad v^2 = \frac{v_2 + v_3}{2}, \quad v^3 = \frac{v_3 + \frac{1}{2}}{2}.$$

Then denote

$$\Delta v^1 = v_2 - v_1, \quad \Delta v^2 = v_3 - v_2, \quad \Delta v^3 = 1/2 - v_3, \\ \alpha = \frac{\alpha^0}{v_1} = \frac{2\alpha^1}{\Delta v^1} = \frac{2\alpha^2}{\Delta v^2} = \frac{2\alpha^3}{\Delta v^3}.$$

Besides, denote $\varepsilon = e^{-\alpha T}$. As we consider only large intervals T , ε is implied to be small enough. Find $p(v)$ separately at the intervals $[0, v_1]$, $[v_1, v_2]$, and $[v_2, v_3]$.

1) Let $0 \leq v \leq v_1$.

Here $\dot{v} = -\alpha(v - v_1)$, and the general solution is

$$v = v_1 + (v_0 - v_1)e^{-\alpha t}, \quad 0 \leq v_0 \leq v_1. \quad (16)$$

From (16) express v_0 through v :

$$v_0 = e^{\alpha t} v - v_1(e^{\alpha t} - 1), \quad v_1(1 - e^{-\alpha t}) \leq v \leq v_1.$$

Note that $\frac{\partial v_0}{\partial v} = e^{\alpha t}$. Then (13) gives

$$p(v, t) = \begin{cases} e^{-v_1} e^{\alpha t} e^{(v_1-v)e^{\alpha t}}, & v_1(1 - e^{-\alpha t}) \leq v \leq v_1 \\ 0 & , \quad 0 \leq v \leq v_1(1 - e^{-\alpha t}) \end{cases}.$$

From (14) obtain:

$$p(v) = \begin{cases} \frac{e^{-v_1}}{T} \int_0^{t(v)} e^{\alpha t} e^{(v_1-v)e^{\alpha t}} dt, & 0 \leq v \leq v_{1T} \\ \frac{e^{-v_1}}{T} \int_0^T e^{\alpha t} e^{(v_1-v)e^{\alpha t}} dt, & v_{1T} \leq v \leq v_1 \end{cases}.$$

Where $t(v) = -\frac{1}{\alpha} \ln\left(\frac{-v + v_1}{v_1}\right)$ is the reverse function of (16). Since $\int e^{\alpha t} e^{(v_1-v)e^{\alpha t}} dt = \frac{e^{(v_1-v)e^{\alpha t}}}{\alpha(v_1 - v)}$,

finally obtain:

$$p(v) = \begin{cases} \frac{e^{-v_1}}{\alpha T} \frac{e^{v_1} - e^{v_1-v}}{v_1 - v}, & 0 \leq v \leq v_{1T} \\ \frac{e^{-v_1}}{\alpha T} \frac{e^{(v_1-v)e^{\alpha T}} - e^{v_1-v}}{v_1 - v}, & v_{1T} \leq v \leq v_1 \end{cases}.$$

2) Let $v_1 \leq v \leq v_2$.

Then

$$\dot{v}(v) = \begin{cases} \alpha(-v + v_1), & v_1 \leq v \leq v^1 \\ \alpha(v - v_2), & v^1 \leq v \leq v_2 \end{cases}. \quad (17)$$

Write general solutions separately for the two intervals:

$$v(v_0, t) = v_0 e^{-\alpha t} + v_1 (1 - e^{-\alpha t}), \quad v_1 \leq v \leq v^1 \quad (18')$$

$$v(v_0, t) = v_0 e^{\alpha t} + v_2 (1 - e^{\alpha t}), \quad v^1 \leq v \leq v_2 \quad (18'')$$

Then write the general solution of (17):

$$v(v_0, t) = \begin{cases} v_0 e^{-\alpha t} + v_1 (1 - e^{-\alpha t}), & v_1 \leq v_0 \leq v^1 \\ v^1 e^{-\alpha(t-t_0)} + v_1 (1 - e^{-\alpha(t-t_0)}), & v^1 \leq v_0 \leq v_2, \quad v_1 \leq v \leq v^1, \\ v_0 e^{\alpha t} + v_2 (1 - e^{\alpha t}), & v^1 \leq v \leq v_2 \end{cases} \quad (19)$$

where t_0 is the time of transition from v_0 to v^1 obtained from (18'') by substituting v^1 for v :

$$v^1 = -e^{\alpha t_0} (v_2 - v_0) + v_2, \\ e^{\alpha t_0} = \frac{v_2 - v^1}{v_2 - v_0} = \frac{\Delta v^1}{2(v_2 - v_0)}.$$

Then (19) looks as:

$$v(v_0, t) = \begin{cases} v_0 e^{-\alpha t} + v_1 (1 - e^{-\alpha t}), & v_1 \leq v_0 \leq v^1 \\ \frac{(\Delta v^1)^2 e^{-\alpha t}}{4(v_2 - v_0)} + v_1, & v^1 \leq v_0 \leq v_2, \quad v_1 \leq v \leq v^1. \\ v_0 e^{\alpha t} + v_2 (1 - e^{\alpha t}), & v^1 \leq v \leq v_2 \end{cases}$$

Express v_0 via v :

$$v_0(v, t) = \begin{cases} v e^{\alpha t} - v_1 (e^{\alpha t} - 1), & v_1 \leq v_0 \leq v^1 & (20') \\ v_2 - \frac{(\Delta v^1)^2 e^{-\alpha t}}{4(v - v_1)}, & v^1 \leq v_0 \leq v_2, \quad v_1 \leq v \leq v^1 & (20'') \\ v e^{-\alpha t} + v_2 (1 - e^{-\alpha t}), & v^1 \leq v \leq v_2 & (20''')$$

The constraint $v_1 \leq v_0 \leq v^1$ transforms into $v_1 \leq v e^{\alpha t} - v_1 (e^{\alpha t} - 1) \leq v^1$ or $v_1 \leq v \leq v_1 + \frac{\Delta v^1}{2} e^{-\alpha t}$. The

constraints from (20'') transform into $v_1 + \frac{\Delta v^1}{2} e^{-\alpha t} \leq v \leq v^1$.

$$v_0(v, t) = \begin{cases} v e^{\alpha t} - v_1 (e^{\alpha t} - 1), & v_1 \leq v \leq v_{2T} & (a) \\ v_2 - \frac{(\Delta v^1)^2 e^{-\alpha t}}{4(v - v_1)}, & v_{2T} \leq v \leq v^1 & (b) \\ v e^{-\alpha t} + v_2 (1 - e^{-\alpha t}), & v^1 \leq v \leq v_2 & (c) \end{cases} \quad (21)$$

where $v_{2T} = v_1 + \frac{\Delta v^1}{2} \varepsilon$.

Integration over the areas (a), (b), (c) of the equations for $p(v, t)$ obtained from (12), (13), and (15) gives the following $p(v)$:

$$p(v) = \begin{cases} \frac{e^{-v_1} e^{\frac{v_1-v}{\varepsilon}} - e^{v_1-v}}{\alpha T (v_1 - v)}, & v_1 \leq v \leq v_{2T} \\ \frac{e^{-v_1} e^{-(v-v_1)} - e^{-\Delta v^1} e^{\frac{\beta}{v-v_1}}}{\alpha T (v - v_1)}, & v_{2T} \leq v \leq v^1 \\ \frac{e^{-v_2} e^{v_2-v} - e^{\varepsilon(v_2-v)}}{\alpha T (v_2 - v)}, & v^1 \leq v \leq v_2 \end{cases}$$

In a similar manner for the interval $v_2 < v < v_3$ obtain:

$$p(v) = \begin{cases} \frac{e^{-v_2} e^{-\varepsilon(v-v_2)} - e^{-(v-v_2)}}{\alpha T (v - v_2)}, & v_2 \leq v \leq v^2 \\ \frac{e^{-v_3} e^{\Delta v^2} e^{\frac{(\Delta v^2)^2}{4(v_3-v)} \varepsilon} - e^{v_3-v}}{\alpha T (v_3 - v)}, & v^2 \leq v \leq v_{3T} \\ \frac{e^{-v_3} e^{\frac{v_3-v}{\varepsilon}} - e^{v_3-v}}{\alpha T (v_3 - v)}, & v_{3T} \leq v \leq v_3 \end{cases}$$

Figure 5 shows the plot of function $p(v)$ for large T . At the points of stable equilibrium v_1 and v_3 there are two marked peaks. Note that the actual number of spherical tumours with unstable shapes over $[v_0, v_3]$ is much lower than it would be expected from the above calculations which assumed stability over the whole range of intervals.

4. Conclusion

The reproduction rate of cancer cells is controlled by the local concentrations of interacting cancer and tissue cells, and hence by the curvature of the surface between the tumour and the host tissue. The local concentration of cancer cells increases with the curvature radius. Assumption of non-monotone dependence of reproduction rate vs. local concentration of cancer cells reveals critical values R_{\min} (corresponding to the beginning of spherical tumour growth) and R_{\max} (corresponding to the end of growth). The spherical shape is stable until the radius reaches the value R_0 corresponding to the maximum rate of tumour growth. When the size of the tumour is between R_0 and R_{\max} , its spherical shape becomes unstable as a minor casual deformation triggers the faster reproduction of cancer cells at the sites where the curvature radius approaches R_0 . Then the tumour transforms into an ellipsoid, elongated outgrowths, or a branching structure, which occasionally cause the detachment of metastases at the sites of negative curvature. As tumours grow at different rates through their evolution stages, it is possible to estimate the statistical distribution of their sizes and shapes.

We wish to thank Yu. Sharovskaya who drew R. Kh's attention to the role of local cellular interactions in the reproduction of cancer cells.

References

- [1] J. Adam, A simplified model of tumor growth, *Math. Biosci.* 81 (1986) 229-244.
- [2] J. Adam, A mathematical model of tumor growth. II. Effects of geometry and spatial nonuniformity on stability, *Math. Biosci.* 86 (1987) 183-211.
- [3] J. Adam, A mathematical model of tumor growth. III. Comparison with experiment, *Math. Biosci.* 86 (1987) 213-227.

- [4] R. Wasserman, R. Acharya, C. Sibata, and K. Shin, A patient-specific in vivo tumor model, *Math. Biosci.* 13 (1996) 111-140.
- [5] A. Kopp-Shneider and C. Portier, A stem cell model for carcinogenesis, *Math. Biosci.* 120 (1994) 211-232.
- [6] A. Dewanji, S. Moolgavkar, and E. Luebeck, Two-mutation model for carcinogenesis: joint analysis of premalignant and malignant lesions, *Math. Biosci.* 104 (1991) 97-109.
- [7] N. Bellomo, G. Forni, Dynamics of tumor interaction with the host immune system, *Mathl. Comput. Modelling.* Vol. 20, No. 1 (1994) 107-122.
- [8] C. Calderon and T. Kwembe, Modeling tumor growth, *Math. Biosci.* 103 (1991) 97-114.
- [9] S. Michelson and J. Leith, Unexpected equilibria resulting from differing growth rates of subpopulations within heterogeneous tumors, *Math. Biosci.* Vol. 91 (1988) 119-129.
- [10] M. Orme and M. Chaplain, A mathematical Model of vascular tumour growth and invasion, *Mathl. Comput. Modelling.* Vol. 23, No. 10 (1996) 43-60.
- [11] W. Kendal, The role of multiple somatic point mutations in metastatic progression, *Math. Biosci.* 108 (1992) 81-88.
- [12] Ž. Bajzer, M. Marušić, and S. Vuk-Pavlović, Conceptual frameworks for mathematical modelling of tumor growth dynamics, *Mathl. Comput. Modelling.* Vol. 23, No. 6 (1996) 31-46.
- [13] Gleiberman A.S., Kudrjavitseva E.I., Sharovskaya Yu. Yu., Abelev G.I., Synthesis of alpha-fetoprotein in hepatocytes is co-ordinately regulated with cell-cell and cell-matrix interactions. *Mol. Biol. Med.*, Vol. 6 (1989) 95-107.
- [14] Sharovskaya Yu. Yu., Chailakhjan L.M, Local cell interaction and cell growth control, *Doklady Biochemistry.* Vol. 366 (1999) 80-83.
- [15] Sharovskaya Yu.Yu., Gainulina S.M., Yakusheva A.A., Kordyukova L.V., Chailakhjan L.M., Aleksandrov V.B., Organoid culture of human colon adenocarcinoma as a model of local intercellular interactions, *Biological Science*, Vol. 377 (2001) 187-190.
- [16] M. Abercrombie, Contact inhibition and malignancy, *Nature (London).* Vol. 281 (1979) 259-262.
- [17] Jongen W.M., Fitzgerald D.J., Asamoto M., Piccoli C., Slaga T.J., Cros D., Takeichi M., Yamasaki H., Regulation of connexin 43-mediated gap junctional intercellular communication by Ca^{2+} in mouse epidermal cells is controlled by E-cadherin, *J. Cell Biol.* Vol. 114. No. 3 (1991) 545-555.
- [18] Deutsch E., Libson K., Vanderheyden J.-L., Ketring A.R., Maxon H.R., *Nucl. Med. Biol.*, 1986,v.13, p. 465
- [19] Jurisson S., Berning D., Jia W., Ma D., *Chem. Rev.*, 1993, v.93, p. 1137
- [20] Dilworth J.R., Parrott S. J., *Chem Soc. Rev.*, 1998, v.27, p. 43-55.
- [21] Heeg M.J., Jurisson S.S., *Acc. Chem. Res.*, 1999, v.32, p.1053-1060.

Figure captions

Fig. 1. Reproduction rates of cancer cells \dot{v} as a function of their local concentration v (curves 1-3).

Fig. 2. Derivative of cancer cells density at the tumour surface $\psi(v)$ (solid line), and initial reproduction function $\varphi(v)$ (dashed line).

Fig. 3. Growth and formation of tumour at minor deformations. Dashed line shows a deformed tumour, solid line shows tumour shape some time after deformation. Arrows show the magnitude and direction of tumour growth in the corresponding points. (a) The initial tumour has a curvature radius between R_2 and R_0 . (b) The initial tumour has a curvature radius between R_0 and R_3 . (c) Curvature radius on the end of the "ellipsoid" exceeds R_0 . (d) Curvature radius at the end of the outgrowth is less than R_0 . (e) Detachment of the outgrowth in a site of negative curvature. (f) Detachment of the outgrowth from the main tumour and development of a metastasis.

Fig. 4. Piecewise linear function $\dot{v} = \chi(v)$ used as approximation for $\psi(v)$.

Fig. 5. Probability density describing statistical distribution of tumours in a tissue.

FIGURE 1

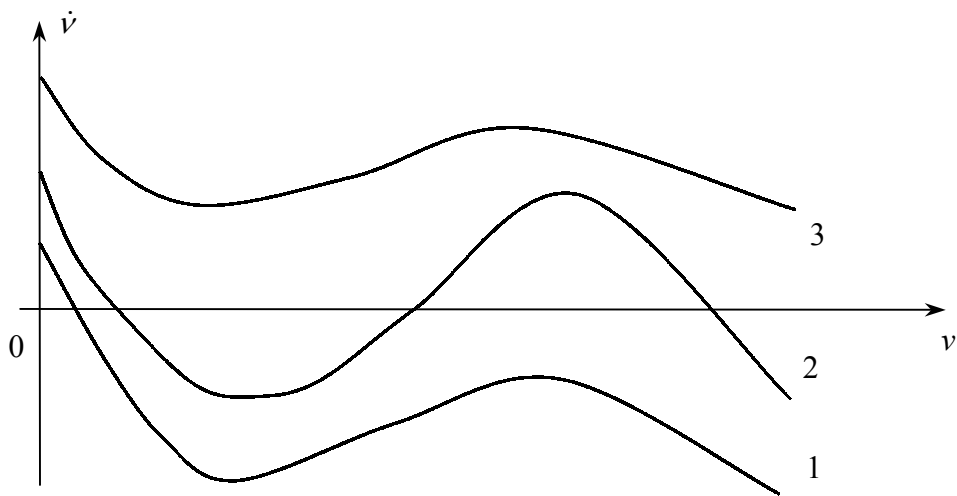


FIGURE 2

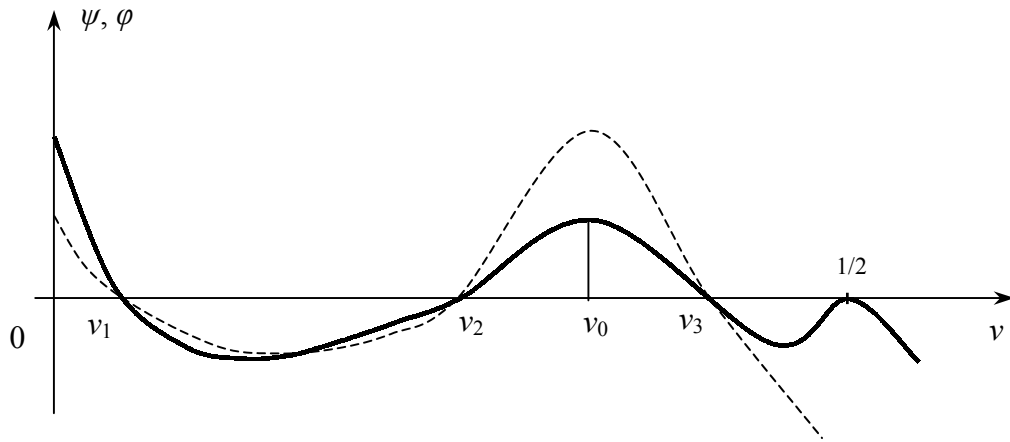


FIGURE 3a

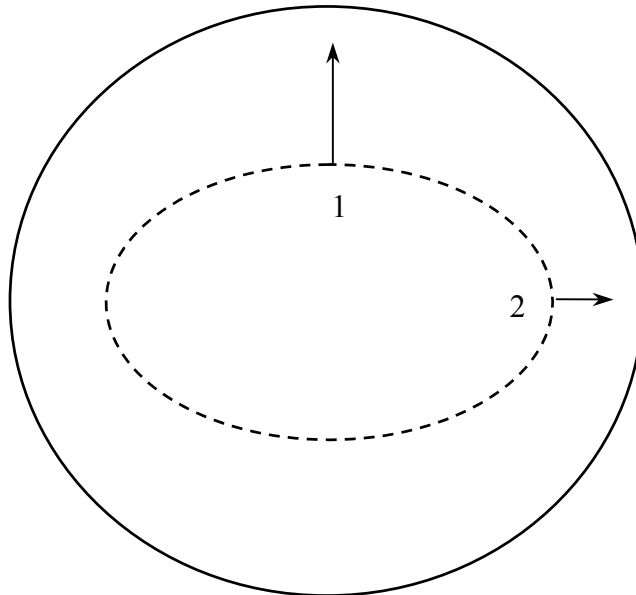


FIGURE 3b

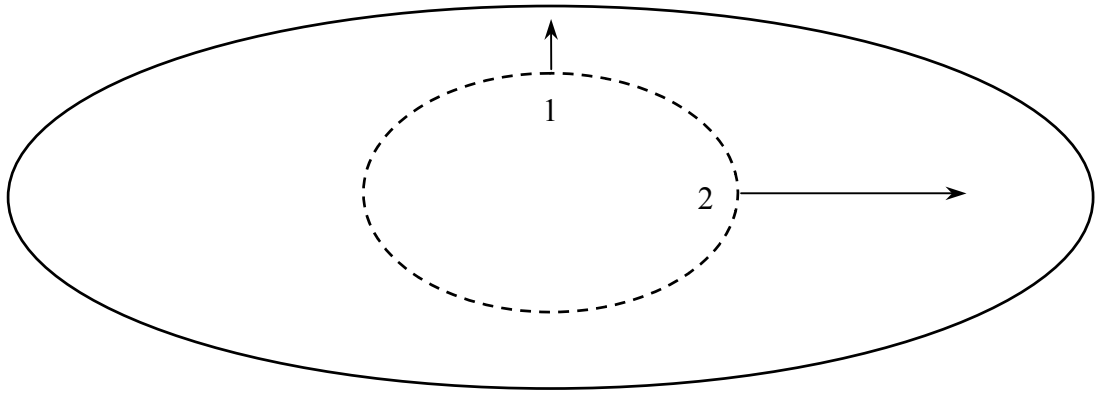


FIGURE 3c

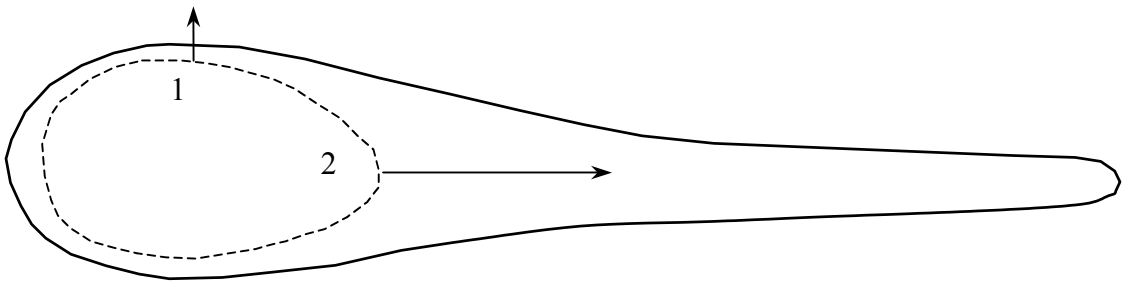


FIGURE 3d

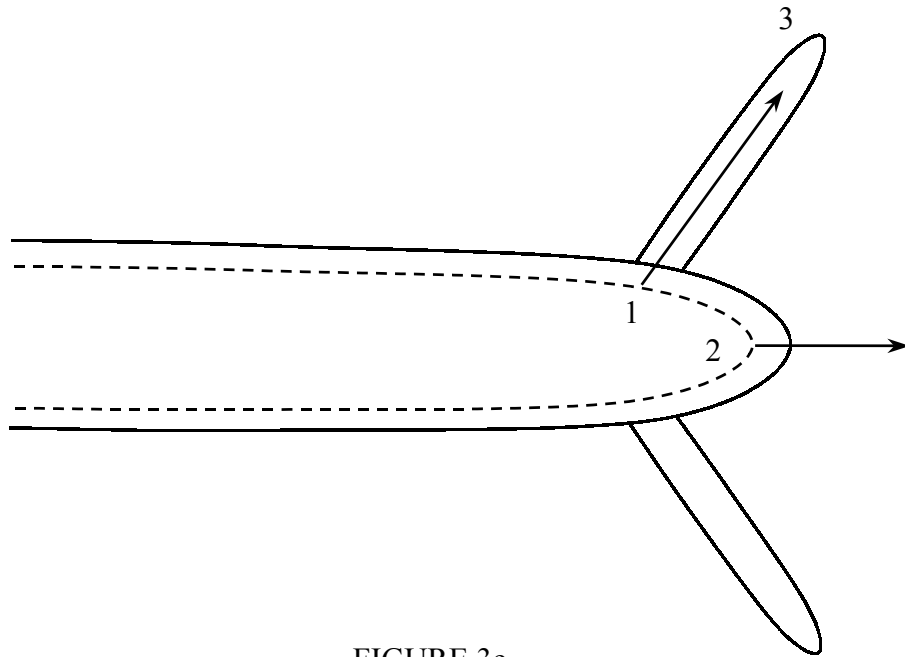


FIGURE 3e

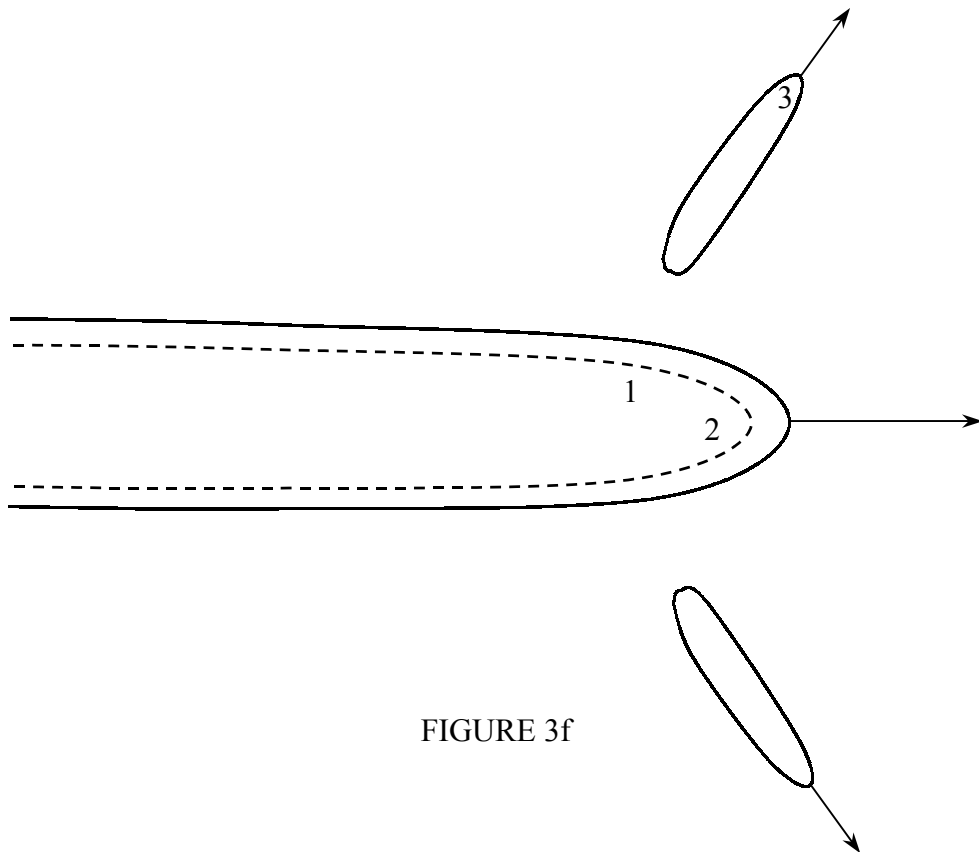


FIGURE 3f

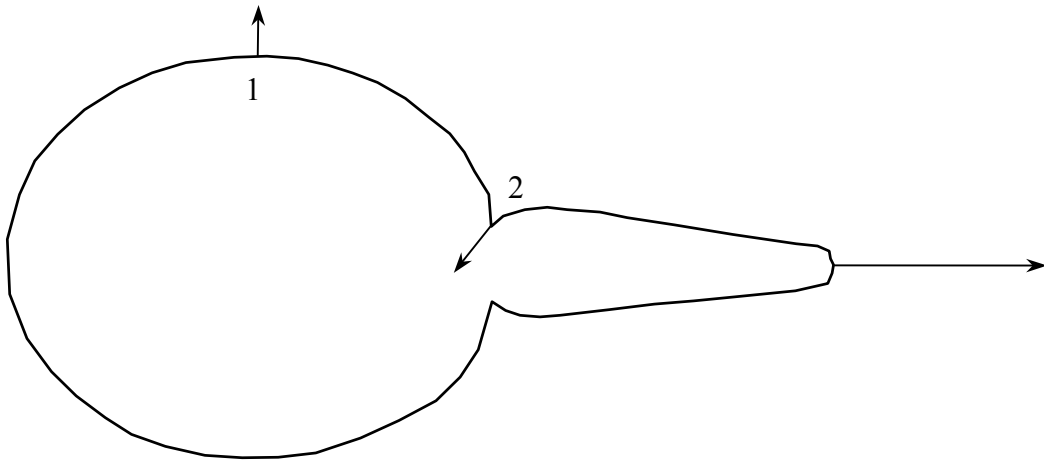


FIGURE 4

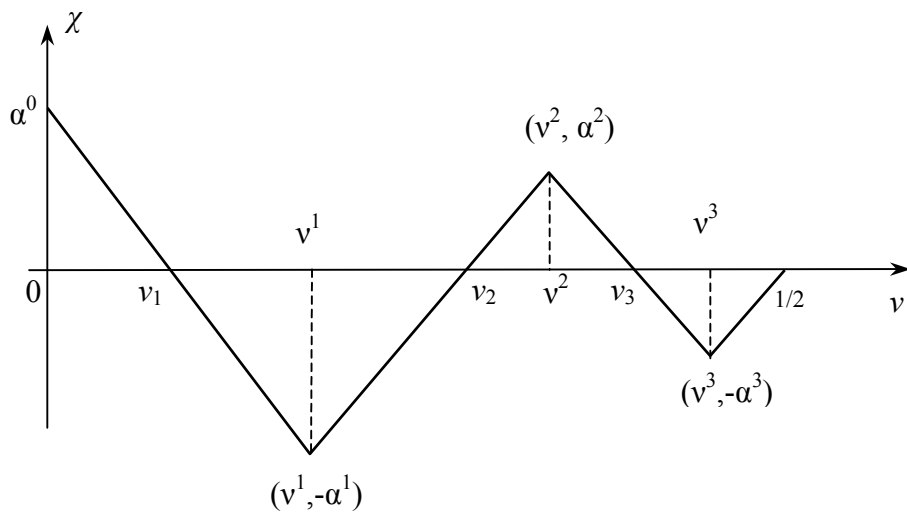


FIGURE 5

